Trabalho apresentado no XLI CNMAC, Unicamp - Campinas - SP, 2022.

Proceeding Series of the Brazilian Society of Computational and Applied Mathematics
Preprint

A mollified version of the Kuwabara-Kono model for 2nd order convergence in DEM

Gabriel Nóbrega Bufolo[1], Yuri Dumaresq Sobral[2]
UnB, Brasília, DF

Abstract. The discrete element method is a technique widely used to simulate multi particle systems, in particular granular materials. For conservative systems, the integration of the equations of motions is often performed via a Verlet-type method of order two. However, when dissipative forces are included, such as in simulations of granular materials, the Verlet method no longer behaves as a second order method. For instance, when using the popular Kuwabara-Kono force scheme, the order of the Verlet method decreases to 1.5. In this work, we propose a regularization of the Kuwabara-Kono force model via mollification. We show numerically that the Verlet method combined with this regularized force model can integrate collisions with second order accuracy and that the coefficient of restitution of the system tends to increase as a function of the regularization parameter.

Keywords. Discrete Element Method, Verlet Method, Kuwabara-Kono Model, Mollifiers

1 Introduction

Consider two spherical particles, say P_1 and P_2, in a plane perpendicular to the direction of gravity, in such a way that they will evolve to a purely normal collision. In this case, the collision is free of any tangential forces and the motion of the particles is governed by Newton's second law of motion. The DEM algorithm provides a way to determine the contact force by establishing a relationship between the force and the overlap $\xi(t)$ between the two particles, defined as

$$\xi(t) = R_1 + R_2 - |\mathbf{x}_1(t) - \mathbf{x}_2(t)|, \tag{1}$$

where R_i and $\mathbf{x}_i(t)$ denotes, respectively, the radius and position of the particle P_i, $i = 1, 2$. One of the most frequent force models used in DEM is the Kuwabara-Kono force model [4], which is given by

$$|\mathbf{F}_i(t)| = k\xi(t)^{3/2} + \gamma\xi'(t)\,\xi(t)^{1/2}, \tag{2}$$

where k is related to the stiffness of the material of the particles and γ is the damping constant. This model is widely used because it reproduces very well the behavior of normal collision of real particles [4, 6, 7].

In DEM simulations of granular materials, Newton's second law is usually integrated in time with Verlet methods [3]. When the force depends explicitly on the velocity, however, the Verlet method has to be adapted so that it retains second order accuracy [8]. For an unidimensional motion along the axis defined by the centers of the particles, the adapted method is given by the

[1] gbufolo7@gmail.com
[2] ydsobral@unb.br

following iterative process:

$$\begin{cases} \hat{v}_{n+\frac{1}{2}} &= v_{n-\frac{1}{2}} + F\left(t_n, x_n, v_{n-\frac{1}{2}}\right)\Delta t; \\ \hat{x}_{n+1} &= x_n + \hat{v}_{n+\frac{1}{2}}\Delta t; \\ v_n &= \dfrac{\hat{x}_{n+1} - x_{n-1}}{2\Delta t}; \\ v_{n+\frac{1}{2}} &= v_{n-\frac{1}{2}} + F(t_n, x_n, v_n)\Delta t; \\ x_{n+1} &= x_n + v_{n+\frac{1}{2}}\Delta t; \end{cases} \tag{3}$$

for each of the particles and for $n = 1, \ldots, N$.

In this work, collision simulations were assembled in such a way that both particles have no angular motion and one of the particles is fixed, i.e. its position is not evolved in time. The center of the other particle is placed at a distance $R_1 + R_2$ of the center of the fixed particle, with an initial velocity of magnitude $1\,\mathrm{m/s}$ and in the direction of the fixed particle. The simulation is then allowed to run for $105 \times 2^{-13}\,\mathrm{s}$ ($\approx 1.2 \times 10^{-2}\,\mathrm{s}$). Two such simulations were run, one using the Kuwabara-Kono force model given in eq. 2, with parameters given in table 1, and another one where the purely elastic Hertz force model was used instead, i.e. $\gamma = 0$ in eq. 2. The order of the Verlet method in eqs. 3 was determined for each of the simulations. The results are presented in fig. 1.

Table 1: Values of the material and model parameters used to simulate a binary normal collision between two particles.

Particles	Normal Forces	Simulation
$\rho = 19300\,\mathrm{kg/m^3}$	$\tilde{k}_n \approx 4.4 \times 10^{10}\,\mathrm{N/m^{1.5}}$	$t_f - t_0 = 105 \times 2^{-13}\,\mathrm{s}$
$r = 1\,\mathrm{m}$	$\gamma \approx 1.1 \times 10^{9}\,\mathrm{kg}/\left(\mathrm{m^{0.5}s}\right)$	$\left(\approx 1.2 \times 10^{-2}\,\mathrm{s}\right)$

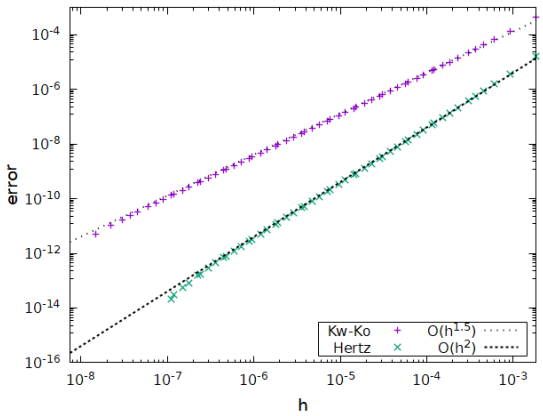

Figure 1: Order analysis of the position of the moving particle involved in the binary normal collision. The values of the parameters can be found in table 1. The usual Hertz model has no damping term, which means that $\gamma = 0$ in eq. 2 in this case.

The results of the order analysis depicted in fig. 1 reveal an unexpected behavior. When the purely elastic force model is used, the accumulated error in the position decreases as $\mathcal{O}(h^2)$, as it is expected when eqs. 3 is used to integrate the motion of the particle. However, when the full Kuwabara-Kono force model is used, the curve approximating the accumulated error in the position decreases as $\mathcal{O}(h^{1.5})$, which does not agree with the expected order of eq. 3.

The inclusion of the dissipation term in the model penalized the order of the Verlet algorithm given by eqs. 3. The cause of this order reduction, therefore, has to lie in the $\xi^{1/2}$ term in eq. 2: at the beginning and in the end of the collision, when $\xi = 0$, the derivative of the term $\xi^{1/2}$ becomes unbounded. It seems that this issue has not yet been observed nor discussed in the literature.

2 A regularized force model

In this section, we propose a regularization of the Kuwabara-Kono model given ineq. 2 based on the concept of mollifiers. The proposed regularization removes the unboundedness of the first derivative of $\xi^{1/2}$ near $t = 0$ and allows for an order 2 convergence of the Verlet method.

2.1 Mollifiers

Let $\phi : \mathbb{R} \to \mathbb{R}$ be defined as

$$\phi(x) \coloneqq \begin{cases} \frac{1}{C} \exp\left(\frac{1}{x^2 - 1}\right) & \text{if } -1 < x < 1; \\ 0 & \text{otherwise,} \end{cases} \tag{4}$$

where

$$C \coloneqq \int_{-1}^{1} \exp\left(\frac{1}{x^2 - 1}\right) dx \approx 0.444 \tag{5}$$

is chosen such that the integral of $\phi(x)$ equals 1. The function defined by eq. 4 is called the "standard mollifier". [2].

For any $\epsilon \in (0, \infty)$, one can then define the real function

$$\phi_\epsilon(x) \coloneqq \frac{1}{\epsilon} \phi\left(\frac{x}{\epsilon}\right). \tag{6}$$

Given $f : \mathbb{R} \to \mathbb{R}$ a locally integrable function, one can define its ϵ-mollification as the convolution of ϕ_ϵ and f. This convolution produces a new real function denoted by $\phi_\epsilon * f$ and which is given by:

$$(\phi_\epsilon * f)(x) = \int_{-\epsilon}^{\epsilon} \phi_\epsilon(z) f(x - z) \, dz. \tag{7}$$

The new function originated by eq. 7 has the desired property of being infinitely differentiable in $\mathbb{R}$, while being almost the same function as the original function f. The quality of the approximation of f by $\phi_\epsilon * f$ depends on how small ϵ is taken.

2.2 Extended square root and ϵ-shift

In order to properly calculate the integral in eq. 7, the function f must be defined on $[-\epsilon, \infty)$. In the case of the square root function, which is the one appearing in the dissipation term of eq. 2, this is not true. For this reason, we continuously extend the ordinary square root function to negative numbers by making $\sqrt{x} = 0$ if $x < 0$. This extension is denoted by $\sqrt{\cdot} : \mathbb{R} \to \mathbb{R}$ and will substitute the traditional square root function from now on.

If we use the extended square root function to calculate eq. 6 we observe that the ϵ-mollification of $\sqrt{\cdot}$ is not zero when $x = 0$, as illustrated in fig. 2(a). This could pose a problem for the force model, since it would mean that a non-zero normal force would exist between two particles which

are not in contact. A way to prevent this is to right-shift the function $\sqrt{\cdot}$ by ϵ. That is, for each $\epsilon \in (0, \infty)$, define the right-shift function $\tau_\epsilon : \mathbb{R} \to \mathbb{R}$ as

$$\tau_\epsilon(x) = x - \epsilon. \tag{8}$$

Then, the ϵ-mollification of $\sqrt{\cdot} \circ \tau_\epsilon$, which is depicted in fig. 2(b), is always zero when $x = 0$, i.e. when there is no contact between the particles. For convenience of notation, from now on we define

$$_\epsilon\sqrt{\cdot} := \phi_\epsilon * \left(\sqrt{\cdot} \circ \tau_\epsilon\right). \tag{9}$$

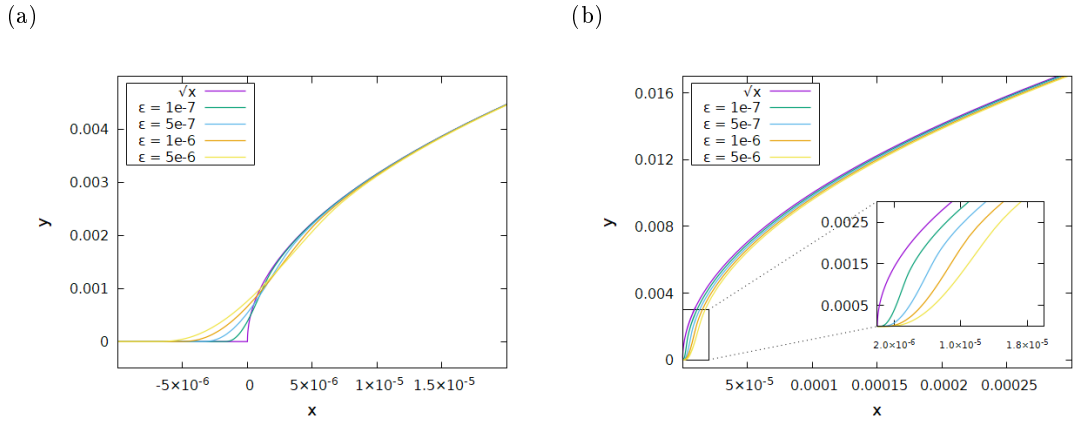

Figure 2: (a) Comparison between $\sqrt{\cdot}$ and the ϵ-mollification of $\sqrt{x}$ for different values of ϵ. (b) Comparison between $\sqrt{\cdot}$ and the ϵ-mollification of $\left(\sqrt{\cdot} \circ \tau_\epsilon\right)$, $_\epsilon\sqrt{\cdot}$, for different values of ϵ. In both plots, the red curve is $\sqrt{x}$, for comparison. Notice how all curves in (b) go through $(0, 0)$. In both figures, mollifications were computed using a composite midpoint rule with 1000 sub-intervals.

2.3 Regularized normal force model

Based on the discussion in the subsections above, we propose a regularized model for the normal contact force in which the $\sqrt{\cdot}$ term in eq. 2 is substituted by $_\epsilon\sqrt{\cdot}$, as defined in eq. 9. Therefore, we obtain

$$|\mathbf{F}_i(t)| = k\xi(t)^{3/2} + \gamma\xi'(t)\,_\epsilon\sqrt{\xi(t)} \tag{10}$$

With the removal of the singularity of the first derivative of $_\epsilon\sqrt{\xi(t)}$ at $t = 0$, the error of the Verlet method given in eqs. 3 should decay as $\mathcal{O}(h^2)$.

We performed simulations for different values of ϵ, in order to evaluate the effect that the mollification parameter has on the overall error behavior. The results are displayed in fig. 3 and indicate that, for all values of ϵ employed, the expected order of the damped Verlet method was recovered, i.e. the error decrease as $\mathcal{O}(h^2)$. In each of the plots in fig. 3, one observes the existence of three distinct regions. The boundary between these regions is highlighted in fig. 3(a). Initially, for larger h, we observe a region where the error, although monotonically decreasing, does not have a clear order, then as h decreases, there is an intermediate region where the relative error oscillates, the length of which seems to depend on ϵ, and finally, for smaller h, a region where the error becomes monotonically decreasing again, but now decreasing as $\mathcal{O}(h^2)$.

The existence of these regions where the error fluctuates can be explained by the observations made in the inset of fig. 2(b), where it is shown that $_\epsilon\sqrt{x}$ and $\sqrt{x}$ are most different when x is

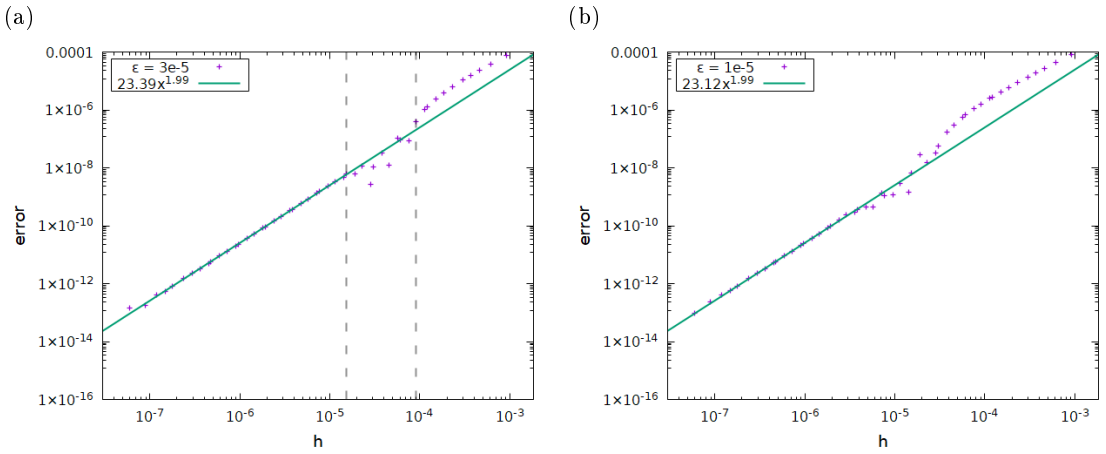

Figure 3: Order analyses of the damped Verlet method associated with the Kuwabara-Kono force model where $\sqrt{\cdot}$ is substituted by ${}_\epsilon\sqrt{\cdot}$. The physical system being simulated is a binary normal collision and the position of one of these particles is the variable whose order is being analyzed. The values of the parameters used in the simulations are presented in table 1.

close to zero. For values of h larger than about 2ϵ, the behavior of ${}_\epsilon\sqrt{x}$ near 0 is never relevant since, in the first step of the integration, the particle will already have crossed the region where ${}_\epsilon\sqrt{x}$ deviates the most from $\sqrt{x}$. Thus, ${}_\epsilon\sqrt{x}$ is effectively very close to $\sqrt{x}$ and the model in eq. 10 behaves almost as the original Kuwabara-Kono model in eq. 2. This is behind the rightmost regions of the plots in fig. 3. However, as h becomes significantly smaller than 2ϵ, i.e. the leftmost regions in fig. 3, the collision of the particles is very well resolved, that is, there will be many time steps in the region of ${}_\epsilon\sqrt{x}$ near 0, which means that the integration of the forces near 0 will be well resolved. In these left-most regions, the $\mathcal{O}(h^2)$ convergence as $h \to 0$ is observed. Finally, for intermediary values of h, the integration of the forces will not sample ${}_\epsilon\sqrt{x}$ near 0 enough times, which causes the erratic behavior observed in the middle region of fig. 7(a).

Therefore, in order to effectively use the regularized model proposed in eq. 10, it is necessary that the value of h belongs to the leftmost region of the plots in fig. 3, for the chosen value of ϵ. Thus, an adequate combination of ϵ and h must be selected. To quantitatively understand how this selection must be made, we performed order analyses for values of ϵ ranging from 5×10^{-7} to 9×10^{-5}. The values of h used in these order analyses were of the form $m \times 2^{-k}$, where $m \in \{1, 3, 5, 7, 15, 21, 35, 105\}$ and $k \in \mathbb{N} \cap [13, 27]$. We choose these values of m so that h is exactly represented as a double precision floating point number, while the total integration time, which must divide all of the possible values of h, is kept relatively low. For each of these analyses, we selected the biggest value of h, called h_ϵ, such that the error decreases as $\mathcal{O}(h^2)$ for all $h < h_\epsilon$. The results are presented in fig. 4. Any pair (ϵ, h_ϵ) below the solid line is a valid choice for which the regularized model in eq. 10 integrated with eqs. 3 will produce an (expected) $\mathcal{O}(h^2)$ decay of the error.

3 Conclusion

In this work, we have identified that, contrary to the expected, the order of the Verlet method, widely used in DEM simulations of granular materials, is not 2 when the model for the normal force used is the Kuwabara-Kono force model. Instead, the convergence of the Verlet method has

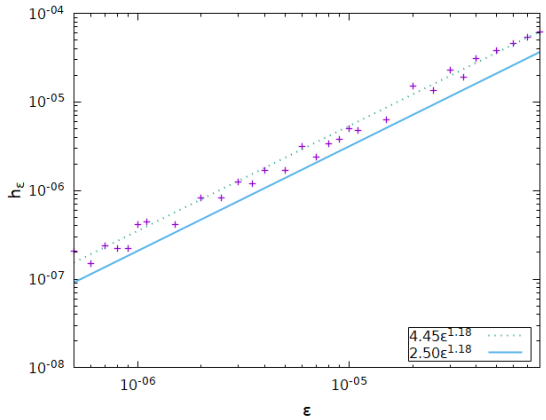

Figure 4: Computed value of h_ϵ as a function of ϵ. The dashed line is the best fit of the data to a power law, while the solid line is "safe" choice for h based on all values of ϵ tested. The values of the parameters used in the simulations are presented in table 1.

order 1.5. This is due to the fact that, in this model, there is a square-root factor linked to the dissipative term that has a singular derivative at the beginning and in the end of particle collisions.

We have proposed a regularized force model, based on an extension of the Kuwabara-Kono model, in which the square-root function appearing in the dissipation term is replaced by a mollified square-root function. This mollified function, which is infinitely differentiable, allows for an actual order 2 integration of the equations of motion in DEM with the Verlet method.

Acknowledgments

This study was partially financed in part by the Coordenação de Aperfeiçoamento de Pessoal de Nível Superior - Brasil (CAPES) - Finance Code 001 (GNB), by the Conselho Nacional de Desenvolvimento Científico e Tecnológico - Brasil (CNPq) (GNB) and by FAP-DF Brazil Project 00193-00000229/2021-21 (YDS, GNB).

References

[1] Eduardo M.B. Campello. "A computational model for the simulation of dry granular materials". In: **International Journal of Non-Linear Mechanics** 106 (2018), pp. 89–107. ISSN: 0020-7462. DOI: https://doi.org/10.1016/j.ijnonlinmec.2018.08.010. URL: https://www.sciencedirect.com/science/article/pii/S0020746218301409.

[2] Lawrence C. Evans. **Partial differential equations**. Providence, R.I.: American Mathematical Society, 2010. ISBN: 9780821849743 0821849743.

[3] Ernst Hairer, Christian Lubich, and Gerhard Wanner. "Geometric numerical integration illustrated by the Störmer–Verlet method". In: **Acta Numerica** 12 (2003), pp. 399–450. DOI: 10.1017/S0962492902000144.

[4] Goro Kuwabara and Kimitoshi Kono. "Restitution Coefficient in a Collision between Two Spheres". In: **Japanese Journal of Applied Physics** 26.Part 1, No. 8 (Aug. 1987), pp. 1230–1233. DOI: 10.1143/jjap.26.1230. URL: https://doi.org/10.1143/jjap.26.1230.

[5] Gustavo H. B. Martins et al. "Large-deviation quantification of boundary conditions on the Brazil nut effect". In: **Phys. Rev. E** 103 (6 June 2021), p. 062901. DOI: 10.1103/PhysRevE.103.062901. URL: https://link.aps.org/doi/10.1103/PhysRevE.103.062901.

[6] J. Shäfer, S. Dippel, and D. Wolf. "Force Schemes in Simulations of Granular Materials". In: **Journal de Physique I** 6.1 (1996), pp. 5–20. DOI: 10.1051/jp1:1996129. URL: https://hal.archives-ouvertes.fr/jpa-00247176.

[7] A.B. Stevens and C.M. Hrenya. "Comparison of soft-sphere models to measurements of collision properties during normal impacts". In: **Powder Technology** 154.2 (2005), pp. 99–109. ISSN: 0032-5910. DOI: https://doi.org/10.1016/j.powtec.2005.04.033. URL: https://www.sciencedirect.com/science/article/pii/S0032591005001658.

[8] Jos Thijssen. **Computational Physics**. 2nd ed. Cambridge University Press, 2007. DOI: 10.1017/CBO9781139171397.

[9] Haruo Yoshida. "Construction of higher order symplectic integrators". In: **Physics Letters A** 150.5 (1990), pp. 262–268. ISSN: 0375-9601. DOI: https://doi.org/10.1016/0375-9601(90)90092-3. URL: https://www.sciencedirect.com/science/article/pii/0375960190900923.

